RSC Advances

PAPER

View Article Online
View Journal | View Issue

Cite this: *RSC Adv.*, 2017, **7**, 25488

Investigation into the pharmacokinetic–pharmacodynamic model of *Zingiberis Rhizoma*/*Zingiberis Rhizoma Carbonisata* and contribution to their therapeutic material basis using artificial neural networks

Sujuan Zhou, [ab] Jiang Meng*[c] and Bo Liu*[a]

Zingiberis Rhizoma (ZR) and *Zingiberis Rhizoma Carbonisata* (ZRC) are two varieties of processed ginger, which are widely used in traditional Chinese medicine (TCM) and exhibit varying drug efficacy. In this study, an Artificial Neural Network (ANN) model was developed for simultaneously characterizing the pharmacokinetics (PK) and pharmacodynamics (PD) of ZR/ZRC. In order to evaluate the relative contribution of the ZR/ZRC drug concentration of its main components to its drug efficacy, connection weights method and Mean Impact Value (MIV) have been introduced. The results have shown that sequences of the contribution value calculated by these two methods was same overall and indicated that the active components of ZR and ZRC exhibited opposite drug efficacy after processing. In conclusion, ANN was found to be a powerful tool that linked PK and PD profiles of ZR/ZRC with multiple components; it also provided a simple method to identify and rank the relative contribution of each to the multiple therapeutic effects of the drug.

Received 5th February 2017
Accepted 27th April 2017

DOI: 10.1039/c7ra01478c

rsc.li/rsc-advances

Introduction

Zingiberis Rhizoma (ZR, Ganjiang) is a well-known herbal medicine and edible plant extensively used in China, India and other South-Eastern Asian countries since thousands of years.[1,2] It is the dried rhizome of *Zingiber officinale Rosc*. *Zingiberis Rhizoma Carbonisata* (ZRC) is produced by stir-frying ZR in a utensil and heating to a temperature that is high enough to turn the bark's surface black-brown.[3,4] According to the TCM theory, ZR has the effect of warming and dispelling cold, venation restoration and warming the lungs to reduce watery phlegm. It can be used to cure cold, vomiting, diarrhea, coughs, *etc.* While ZRC has the function of warming meridian and hemostasis, so it is used for hemorrhage of deficiency cold, hematochezia, metrorrhagia, and metrostaxis.[3,5,6]

The study of pharmacokinetic (PK)–pharmacodynamic (PD) characteristics of ZR and ZRC is to investigate the mechanism of their pharmacodynamics and therapeutics.[7] For traditional Chinese medicines containing multiple components and therapeutic targets,[8,9] the process of developing PK–PD models represents a formidable task and may face methodologic difficulties.[10] Conventional researches on PK–PD mostly rely on known models. That is, PK–PD data should be processed based on the established models and then results could be used in turn to correct the models. This would consume time and money.[11] In contrast, ANN models have lower inaccuracy, cost, and time-consumption.[12,13]

In recent years, Artificial Neural Network (ANN) has been used extensively in the PK–PD analysis model of Chinese herbals for its non-linear fitting ability.[14,15] Without any supposed model, ANN can help to approach a mathematical model[16] reflecting the inherence regularity of experimental data after several times of iterative computation based on the relationship between input and output data. There are different structure types of ANN, in which Back-Propagation (BP)[17] and Radical Basis Function (RBF)[18,19] are the two most widely used methods.[20] Moreover, General Regression Neural Network (GRNN)[21,22] is an improved method of RBF. Herein, we utilized a PK/PD model of ZR/ZRC based on BP and GRNN by selecting time as the correlation factor of drug concentration and efficacy. Furthermore, the relationships between drug concentration of main components and drug efficacy indexes such as TXB2/6-keto-PGF1α and Thromboxane B2 (TXB2) can be analyzed with the aid of this model.

But determining the contribution of each independent variable in ANN models still remains unanswered. Neural network technique is cited in the literature as a 'Black Box'[23] approach and is often criticized for lack of interpretability of the network weights obtained during the model building process.

[a]*Department of Automation, Guangdong University of Technology, Guangzhou, 510006, China. E-mail: csbliu@189.cn; Tel: +86 020 39322469*

[b]*College of Medical Information Engineering, Guangdong Pharmaceutical University, Guangzhou, 510006, China. E-mail: susona2002@163.com; Tel: +86 020 39352207*

[c]*College of Traditional Chinese Medicine, Guangdong Pharmaceutical University, Guangzhou, 510006, China. E-mail: jiangmeng666@126.com; Tel: +86 020 39352169*

This arises from the fact that internal characteristics of a trained network is a set of numbers, which becomes very difficult to relate to the application in a meaningful fashion.[24] Considering this problem, methods to determine the relative importance of variables in a neural network model have been proposed and applied by numerous authors in several research fields:[25,26] perturb, profile, connection weights and partial derivatives.

One of the most important objectives of this study was to evaluate the relative contribution of ZR/ZRC drug concentration of main components to their drug efficacy. Only considerable reports on neural networks technique are available to explore in this field. In the present study, connection weights method and Mean Impact Value (MIV) have been introduced to assess the importance of axon connection weights and contribution of input variables in ANN. Ultimately, the efficacious material basis and process mechanism of ZR/ZRC can be illuminated.

Data source

All experiments reported in the following section have been performed in compliance with animal protection law of China and institutional guidelines of National Natural Science Foundation of China (NSFC). The institutional committees from Faculty and NSFC panels have approved the experiments reported in the present study. All these data were obtained from the research conducted by the Research Group of Jiang Meng supported by the Project of National Natural Science Foundation of China (No. 81102809).

Male Sprague-Dawley (SD) rats (weighing 300 ± 20 g), purchased from Experimental Animal Center of Guangdong Province, have been divided into four groups, namely black group, model group (deficiency-cold and bleeding rats group), ZR treated animals and ZRC treated animals. Blood was collected at different time after the seventh day administration from rats, such as 0.083 0.25, 0.5, 0.75, 1, 2, 3, 4, 5, 6, 7, 10 and 12 h.

Seven compounds of blood (zingiberone, 6-gingerol, 8-gingerol, 6-ginger-ketone, 6-shogaol, diacetoxy-6-gingerdiol and 10-gingerol) were quantified using high-performance liquid chromatography method. Chromatographic conditions: Shimadzu LC-20AT system with DAD (Shimadzu Corp., Japan) was used for all analyses. Chromatographic separations were carried out at 30 °C on an Ultimate TM XB-C18 column (4.6 × 250 mm, 5 μm). The mobile phase consisted of acetonitrile (A) and water containing 0.1% phosphoric acid (B). The gradient elution program was as follows: 0–10 min, 10% A; 10–20 min, 25% A; 20–45 min, 35% A; 45–80 min, 75% A; 80–90 min, 98% A; 90–95 min, 10% A. The flow rate was 0.6 mL min^{-1} and the injection volume was 20 μL.

At the same time, pharmacodynamics was also evaluated with TXB2/6-keto-PGF1α and TXB2. TXB2/6-keto-PGF1α and TXB2 of rats' serum were determined with enzyme-linked immunoassay detection. The details of the experiment will be published in another study.

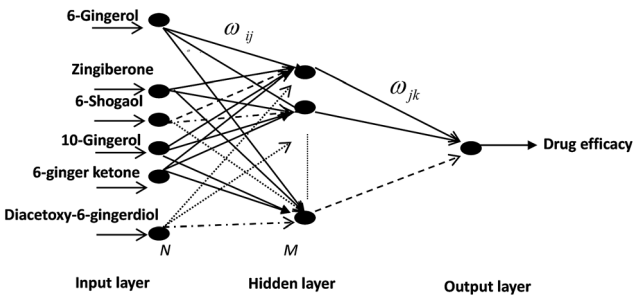

Fig. 1 Structure of the BP neural network used in this study.

PK–PD model construction based on ANN

Construction of BP model

Training datasets and testing datasets. The topological structure of BP neural network is shown in Fig. 1. In this model, contents of 6-gingerol, 8-gingerol (ZR)/zingiberone (ZRC), 10-

Table 1 Training set of PK/PD for ZR[a]

	PK (content/μg ml^{-1})						PD (%)	
Time (h)	6-Gingerol	Zingiberone	6-Shogaol	10-Gingerol	6-Ginger-ketone	Diacetoxy-6-ingerdiol	TXB2/6-keto-PGF1α	TXB2 (%)
0.083	1.292	2.951	0.29	0.479	0.465	0.235	12.875	37.665
0.25	1.484	2.536	1.782	0.309	1.909	0.489	49.235	70.816
0.5	1.618	2.472	2.479	0.203	1.966	1.27	28.287	55.68
0.75	3.116	6.064	3.057	0.556	5.553	0.143	17.379	43.069
1	2.230	7.508	3.52	1.02	3.042	1.387	37.876	63.605
2	2.000	6.385	5.735	0.224	8.691	3.212	64.574	82.703
3	2.135	3.911	4.664	1.01	11.106	2.781	88.714	93.876
4	1.561	2.839	2.67	1.017	8.541	1.998	56.673	77.299
6	1.022	2.276	3.558	0.6	6.69	1.185	63.71	82.703
8	0.739	1.507	3.003	0.229	3.403	0.676	40.101	65.771
10	0.348	1.184	1.81	0.134	1.836	0.798	38.042	63.605
12	0.118	0.322	0.504	0.042	0.977	0.544	22.316	48.474

[a] TXB2/6-keto-PGF1α% = $(C_{\text{treated animals}} - C_{\text{model animal}})/(C_{\text{model animal}} - C_{\text{black animal}}) \times 100\%$. TXB2% = $(C_{\text{treated animals}} - C_{\text{model animal}})/(C_{\text{model animal}} - C_{\text{black animal}}) \times 100\%$.

Table 2 Training set of PK/PD for ZRC[a]

	PK content/μg ml^{-1}						PD (%)	
Time (h)	6-Gingerol	8-Gingerol	6-Shogaol	10-Gingerol	6-Ginger-ketone	Diacetoxy-6-gingerdiol	TXB2/6-keto-PGF1α	TXB2 (%)
0.083	5.011	0.869	0.907	0.95	0.819	1.259	−15.22	−10.4687
0.25	6.746	1.504	1.621	0.65	1.191	1.819	−13.72	−8.8083
0.5	11.718	2.672	2.661	0.983	1.336	0.952	−1.26	−0.5777
0.75	10.148	0.593	3.028	1.352	2.891	1.947	6.16	2.3823
1	8.086	2.994	3.515	2.169	1.787	2.791	−14.84	−10.2522
2	5.842	5.851	4.912	2.006	4.663	2.947	−1.66	−0.2889
3	8.77	4.089	2.35	1.467	6.955	1.646	−6.3	−3.2489
4	7.597	2.507	3.121	1.012	4.463	1.107	−1.42	−0.6496
6	6.228	2.148	3.834	0.455	3.302	0.53	−6.17	−2.8159
8	4.893	0.806	2.694	0.121	2.908	0.52	−14.57	−9.8191
10	1.869	0.169	1.772	0.064	1.719	0.307	−16.17	−11.8403
12	0.271	0	0.908	0.05	0.347	0.152	−16.84	−12.6345

[a] TXB2/6-keto-PGF1α% = $(C_{\text{treated animals}} - C_{\text{model animal}})/(C_{\text{model animal}} - C_{\text{black animal}}) \times 100\%$. TXB2% = $(C_{\text{treated animals}} - C_{\text{model animal}})/(C_{\text{model animal}} - C_{\text{black animal}}) \times 100\%$.

gingerol, 6-shogaol, 6-ginger ketone and diacetoxy-6-gingerdiol were determined as input datasets and corresponding drug efficacy values of TXB2/6-keto-PGF1α and TXB2 were determined as output datasets. To avoid over-fitting, all experimental samples were randomly divided into training datasets and testing datasets by a ratio of five to one. Table 1 shows a group of values of components concentration with TXB2/6-keto-PGF1α

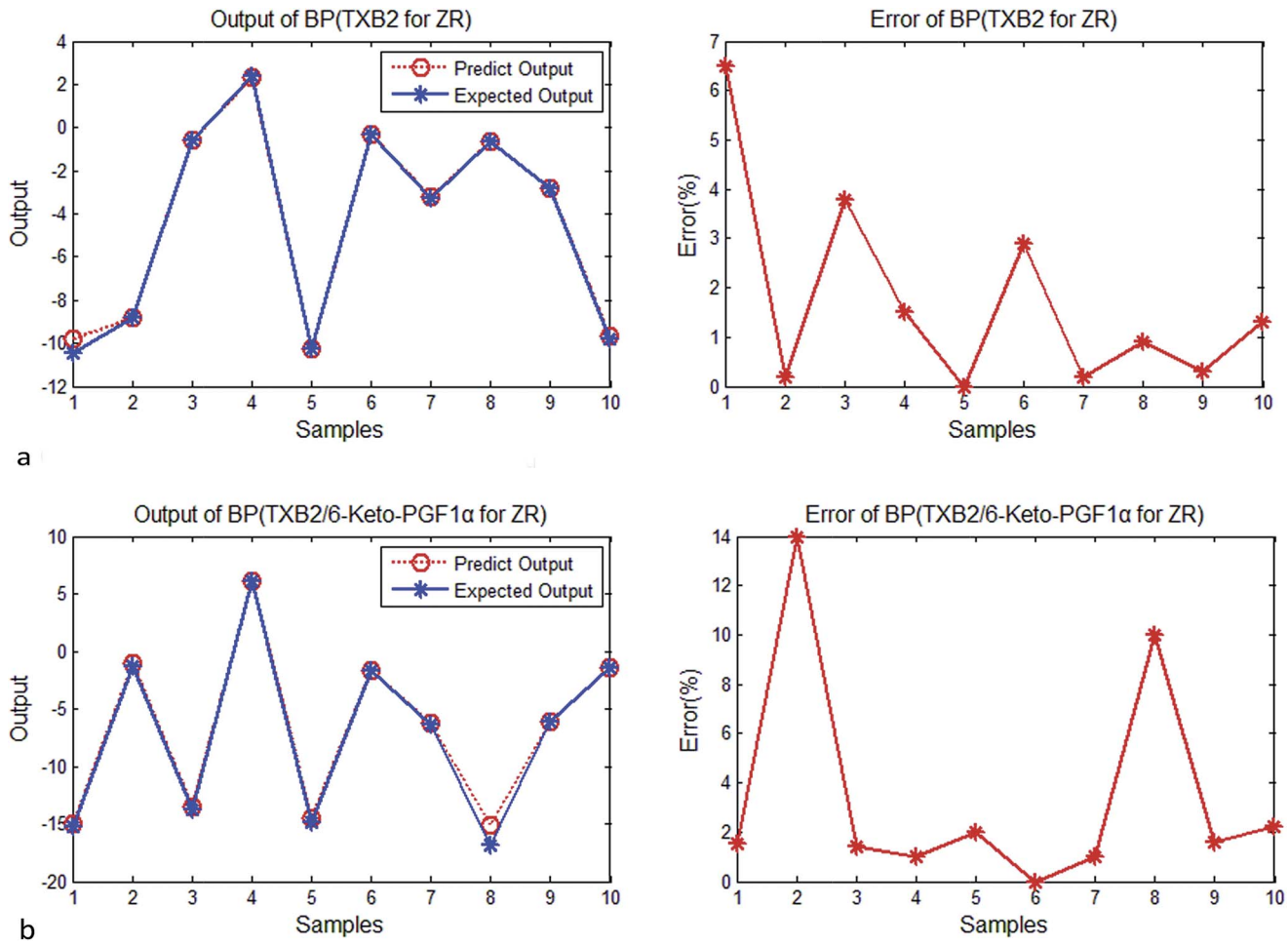

Fig. 2 (a) Output and error of BP (TXB2 for ZR). (b) Output and error of BP (TXB2/6-keto-PGF1α for ZR).

and TXB2 drug efficacy of ZR determined at different time points. Table 2 has shown corresponding values of ZRC.

Selection of hidden-layer neurons number. While constructing BP neural networks, selection of hidden-layer neurons number is very important. It may affect the performance of neural network. Herein, we used an optimization algorithm based on golden section for the number of hidden layer neurons. Repeated experimental results demonstrated that precision was achieved when the hidden-layer neurons number equalled 23 and 16 for model of ZR and ZRC, respectively.

Therefore, selective neural network 6-23-1 topology structure for PK–PD of ZR was determined, where "6" meant six input neurons: 6-gingerol, 8-gingerol, 6-shogaol, 10-gingerol, 6-ginger ketone, diacetoxy-6-gingerdiol, "23" meant hidden-layer neurons number and "1" meant output neurons: values of TXB2/6-keto-PGF1α or TXB2. Similarly, selective neural network 6-16-1 topology structure for PK–PD of ZRC was determined, where "6" meant input neurons: 6-gingerol zingiberone, 6-shogaol, 10-gingerol, 6-ginger, ketone, diacetoxy-6-ingerdiol, "16" meant the hidden-layer neurons number and "1" meant the output neurons: values of TXB2/6-keto-PGF1α or TXB2.

Result of BP network. For ZR and ZRC, two models corresponding to two drug efficacy values of TXB2/6-keto-PGF1α or TXB2 were constructed, programmed by MATLAB R2010a. Herein, training times were set as 2000 epochs and the goal of training errors was set as 0.0001. Fig. 2 and 3 have shown the training results and predicting errors of BP model for ZR and ZRC. From these figures, it was evident that most of the predicting errors were below 10%. Results showed that the predicting model can reflect relationship between the component concentrations and drug efficacy.

Construction of GRNN model. GRNN is one of the most widely used ANN algorithms. It has an advantage of few parameters, with the only threshold that is spread constant SPREAD for the radial basis layer. GRNN was found to be very valuable for interpolation and extrapolation of multivalued functions.[22] A GRNN does not require an iterative training procedure as BP networks. In addition, it was found to be consistent in such a way that as the training set size becomes larger, estimation error approaches zero with only mild restrictions on the function.[27]

Training datasets and testing datasets. GRNN can also be divided into three layers. In the first input layer, the number of neurons is equal to the number of input parameters. In the second hidden layer, number of neurons was equal to the number of training samples, wherein *R* represents net input

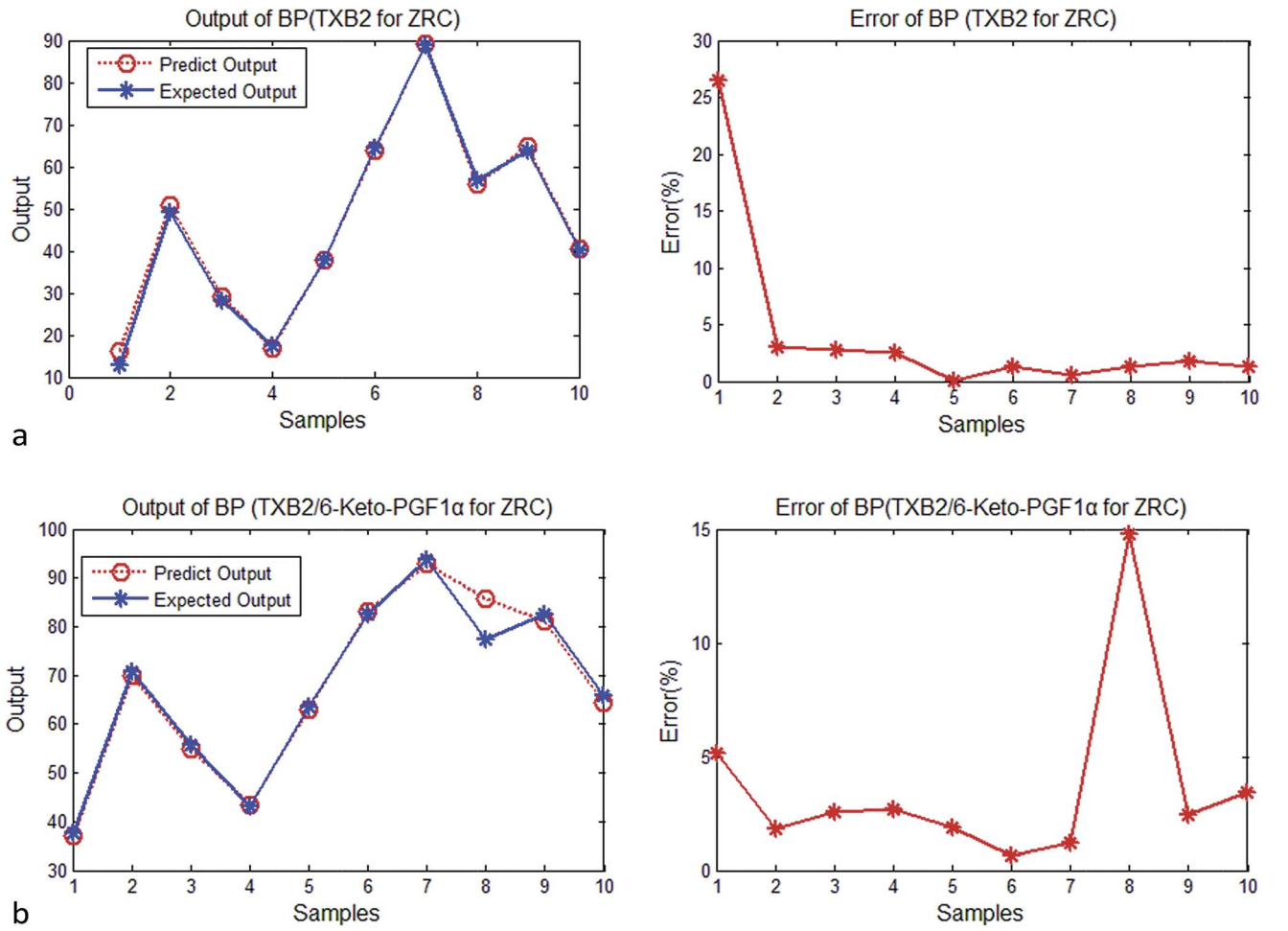

Fig. 3 (a) Output and error of BP (TXB2 for ZRC). (b) Output and error of BP (TXB2/6-keto-PGF1α for ZRC).

dimension and Q represents the neuron numbers for each layer. The transfer function of hidden layer is RBF. Usually, a Gaussian function is used. Smooth factor was included in the transfer function, the smaller of which, better would be the approximation performance. The third layer was the simple output layer. For GRNN, the numbers of RBF neuron, linear neuron and input neuron were the same. The objective of network training was to get appropriate weight matrix and threshold vector.

Learning process. GRNN was generally a supervised learning network. Its learning process included two steps:

The first step was unsupervised learning to determine the weight value IW_1 between input layer and hidden layer; the value of threshold b was determined by the SPREAD constants.

The second step was supervised learning, to generate weight value matrix LW_2 between hidden layer and output layer.

Result of GRNN network. For training, datasets were limited as it might lead to inaccurate results. Then, cross validation methods were used in the experiments to train GRNN network and circuit training was used to find the best value of SPREAD. Programming by MATLAB R2010a, training results and predicting errors of GRNN model for ZR and ZRC have been shown in Fig. 4 and 5.

Comparison of performance between BP and GRNN. As observed in Table 3, on comparing experimental results of BP and GRNN network by average error, the predicting effect of BP network was found to be slightly better. However, GRNN network has advantages of fewer parameters and fast convergence. On the other hand, as the hidden layer neurons of GRNN equals to that of the samples and the quantity related to the latter research was too large, BP network was chosen for further study, to determine relationships between drug concentration of main components and drug efficacy indexes with the aid of PK–PD model.

Evaluation of relative contributions

Based on above results, PK–PD model constructed using neural networks can effectively predict the relationship between component concentrations and drug efficacy. However, one of the limitations of ANN was its high inability to explicitly know the relations between explanatory variables (input) and dependent variables (output). This was a major reason for them being called as "black boxes".[28] In this study, we further explored the relationship between input values and output values, in order to determine the contribution of ZR/ZRC drug concentration of main components to their drug efficacy.

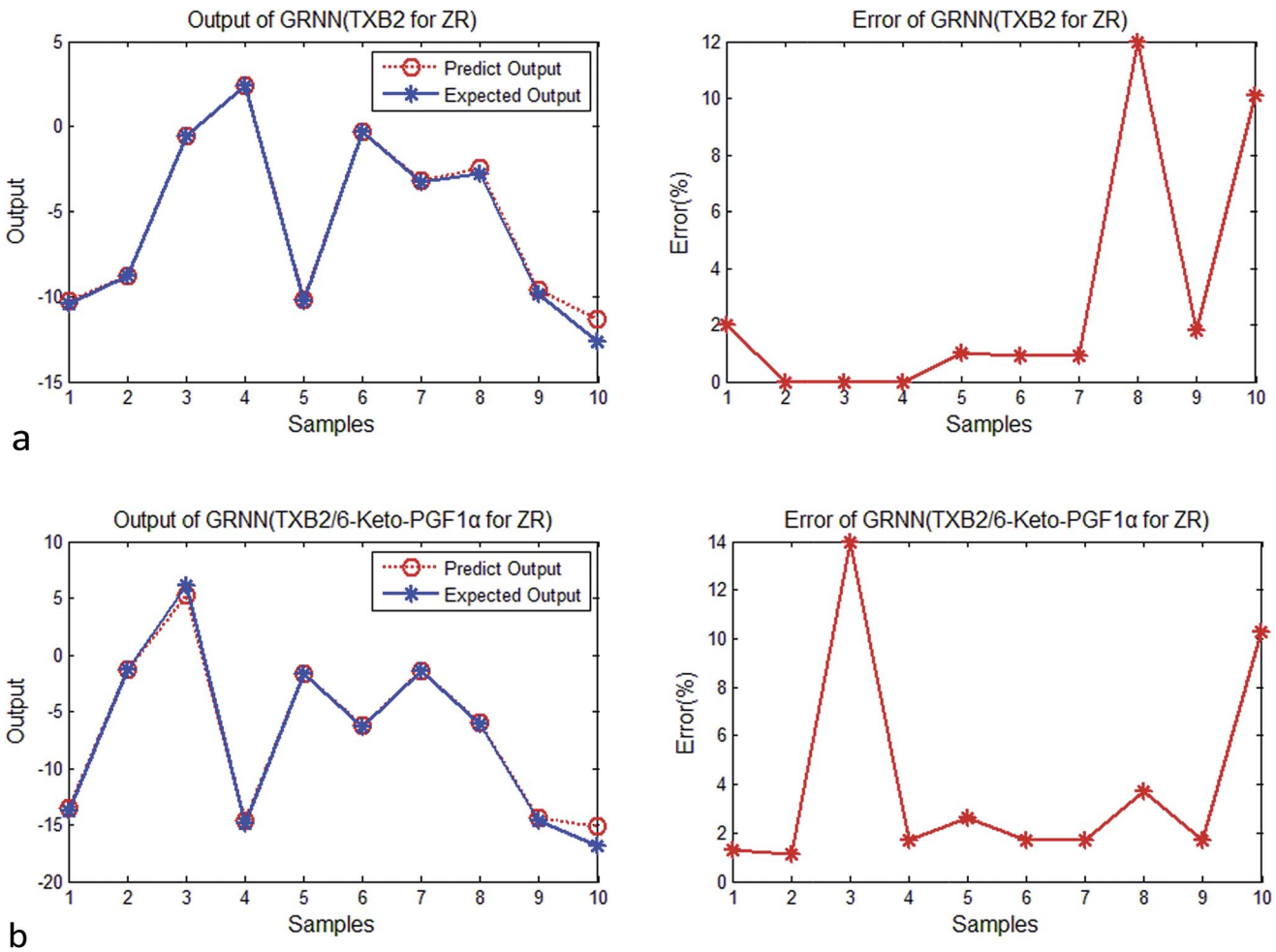

Fig. 4 (a) Output and error of GRNN (TXB2 for ZR). (b) Output and error of GRNN (TXB2/6-keto-PGF1α for ZR).

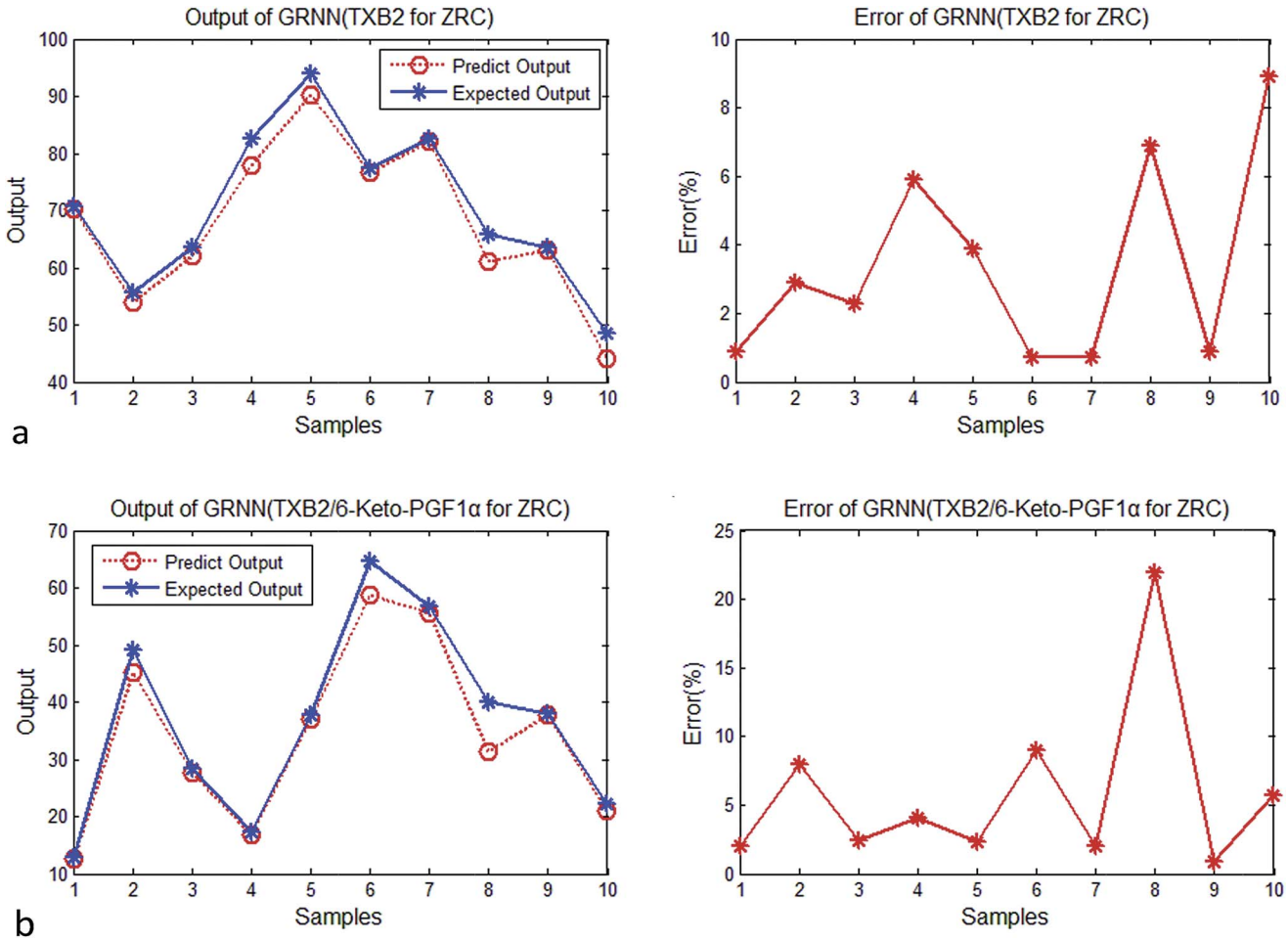

Fig. 5 (a) Output and error of GRNN (TXB2 for ZRC). (b) Output and error of GRNN (TXB2/6-keto-PGF1α for ZRC).

Table 3 Performance compare of BP and GRNN (TXB2 for ZR for example)

	BP	GRNN
Average error	3.6%	3.9%
Parameter numbers	5 (or more)	1
Hidden layer neurons	23	Big (equal to nums of train samples)

For this, connection weights method and Mean Impact Value (MIV) were utilized to solve these problems.

Connection weights method

Connection weights method includes four indexes:[26] matrix containing input-hidden-output neuron connection weights, connection weights contribution value of input-hidden-output layer, relative contribution of each input neuron to the hidden neuron and relative importance of each input variable.

Based on Fig. 6, detailed algorithm of connection weights method has been given as follows:[29,30]

Step 1. Get matrix containing input-hidden-output neuron connection weights in the format shown below.

	Hidden *A*	Hidden *B*
Input 1	W_{A1}	W_{B1}
Input 2	W_{A2}	W_{B2}
Input 3	W_{A3}	W_{B3}
Output	W_{YA}	W_{YB}

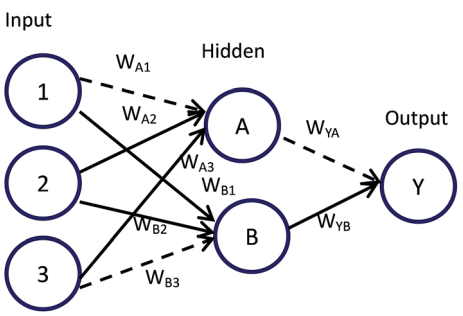

Fig. 6 Garson's algorithm for partitioning and quantifying neural network connection weights.

Step 2. Calculate connection weights contribution value C_{ij} of input-hidden-output layer. C_{ij} means contribution of each input neuron to the output *via* each hidden neuron.

$$C_{ij} = W_{ij} \times W_{Yi},\ i = A,\ B;\ j = 1,\ 2,\ 3$$

where W_{ij} is the synaptic connection weight between the input neuron j and the hidden neuron i, and W_{Yi} is the synaptic weight between the hidden neuron i and the output neuron Y.

Step 3. Calculate total contribution OI_j of each input neuron to the output neuron. OI_j shows the relative contribution of each input variable to output variable, where signs of plus (+) denote positive function and minus (−) denote negative.

$$\mathrm{OI}_j = \sum_{i=A}^{B} C_{ij},\ \ j = 1,\ 2,\ 3$$

Step 4. Calculate relative importance RI_i of each input variable. Value of RI_i greater than zero means positive function to output variable, less than zero means negative function and equal to zero means no function to output.

$$\mathrm{RI}_i = \frac{\mathrm{OI}_i}{\sum_{i=1}^{3} \left|\mathrm{OI}_i\right|} \times 100\%$$

Mean impact value (MIV)

Mean Impact Value (MIV) is one of the most important indexes evaluating the influence of independent variable on dependent variable. It was introduced by Dombi as a method to study ANN for the selection of variables.[31] MIV was used to reflect the changing of weight matrix value in ANN and regarded as one of the best criteria in evaluating correlation of variables. The signs plus (+) or minus (−) denote relevant direction of function and absolute value of MIV value, which means the degree of influence to function. The detailed procedure has been given below:[32]

Step 1. After termination of network training, each independent variable of training sample P are increased by 10% and reduced by 10%. Thus, it constructs two new training samples, P1 and P2.

Step 2. P1 and P2 act as samples to simulate using the constructed network. Now, get two simulation results, A1 and A2.

Step 3. A1 minus A2, and then acquire impact value IV to output after the variables changes.

Step 4. The mean of IV according to the observation is MIV, which reflects the effect of independent variables on dependent variables.

Following the steps above, we calculated the MIV value of each independent variable in turn. By sorting the variables based on their MIV's absolute values, the influence extent of input features over network results can be identified.

Discussion

Tables 4 and 5 have shown contribution values of ZR/ZRC drug concentration of main components to their drug efficacy. From Tables 4 and 5 we can see that sequences of contribution value

Table 4 Results of RI and MIV for ZR

	TXB2/6-keto-PGF1α			TXB2		
Components	OI	RI	MIV	OI	RI	MIV
6-Gingerol	2.354	28.937	0.25	0.586	8.202	0.216
8-Gingerol	0.546	6.713	0.419	−0.151	−2.111	−0.183
6-Shogaol	−1.18	−14.505	0.052	2.504	35.057	0.819
10-Gingerol	3.562	43.784	1.418	−1.314	−18.397	0.067
6-Ginger-ketone	−0.404	−4.964	−0.154	2.32	32.481	0.134
Diacetoxy-6-gingerdiol	0.089	1.096	0.609	0.268	3.752	0.017

Table 5 Results of RI and MIV for ZRC[a]

	TXB2/6-keto-PGF1α			TXB2		
Components	OI	RI	MIV	OI	RI	MIV
6-Gingerol	−0.946	−14.847	−3.217	0.5	6.427	−1.468
Zingiberone	1.232	19.333	2.05	1.898	24.373	1.389
6-Shogaol	1.76	27.616	1.067	−0.457	−5.866	−1.199
10-Gingerol	−0.622	−9.766	−0.933	1.968	25.276	1.419
6-Ginger-ketone	1.716	26.935	3.224	1.403	18.023	3.159
Diacetoxy-6-ingerdiol	−0.096	−1.504	−0.232	−1.56	−20.035	−2.915

[a] OI_j means relative contribution of each input variable to output variable, RI means relative importance of each input variable, MIV means influence of independent variable on the dependent variable. The signs plus (+) or minus (−) denote relevant direction of function.

calculated by connection weights method and MIV were same overall, which indicated that the results were reliable.

Specifically for ZR, as observed in Table 4, it is evident that components of 6-gingerol, 8-gingerol, 10-gingerol and diacetoxy-6-gingerdiol contributions to TXB2/6-keto-PGF1α are positive; of these, 10-gingerol (43.784%) and 6-gingerol (28.937%) have contributed the greatest. However, for components of 6-shogaol and 6-ginger ketone, contribution rates were found negative. For drug efficacy of TXB2, 6-shogaol, 6-ginger ketone, 6-gingerol and diacetoxy-6-gingerdiol make positive contribution and the first two contribute more, while 8-gingerol and 10-gingerol make negative contribution.

Similarly for ZRC, as observed in Table 5, it is notable that components of zingiberone, 6-shogaol and 6-ginger ketone contributions to TXB2/6-keto-PGF1α are positive, thereby revealing the effective substance. However, for components of 6-gingerol, 10-gingerol and diacetoxy-6-ingerdiol, contribution rates are negative. Moreover, for drug efficacy of TXB2, 6-gingerol, zingiberone, 10-gingerol and 6-ginger ketone make positive contribution and 6-shogaol and 1-diacetoxy-6-ingerdiol make negative contribution.

As observed in Tables 4 and 5, it was not difficult to determine that the active components of ZR and ZRC were opposite. Components of positive effect for ZR led to negative effect for ZRC and *vice versa*. The reason can be attributed to different drug efficacy of ZR and ZRC. As we know, ZR has an effect of promoting blood circulation and anti-clotting; while ZRC has the effect of hemostasis and clotting. Therefore, their drug efficacy will be opposite.

Conclusions

Without requiring structural details, ANN clearly exhibited an advantage over conventional model-dependent methods. In this article, an ANN model was developed to characterize the pharmacokinetics and pharmacodynamics of ZR/ZRC simultaneously. The contents of 6-gingerol, 8-gingerol (ZR), zingiberone (ZRC), 10-gingerol, 6-shogaol, 6-ginger ketone and diacetoxy-6-gingerdiol were determined as input datasets and the corresponding drug efficacy values of TXB2/6-keto-PGF1α and TXB2 were determined as output datasets. Time profiles of these markers were well captured using the ANN model.

In order to interpret the contribution of input variables in the neural network modeling process, connection weights method and MIV are utilized to evaluate the relative contribution of ZR/ZRC drug concentration of main components to its drug efficacy. Simulation experiments have shown that sequences of contribution value calculated by connection weights method and MIV were same overall. Moreover, the final results have shown that active components of ZR and ZRC were opposite for their different drug efficacy after processing. The processing mechanism of this type of traditional Chinese medicine can also be revealed.

ANN has shown to handle sparse data well. It also provides a simple means of modelling complex relationship within experimental data, shedding light on the future PK/PD investigation and contribution evaluation of herbal medicines with multi-component and multi-target. It will surely become a promising tool in the field of drug discovery and development.

Acknowledgements

This study was financially supported by the Project of the National Natural Science Foundation of China (No. 81102809), Project of Guangdong Provincial Administration of Traditional Chinese Medicine (No. 20151266) and Educational Information Technology Project of Guangdong Education Department (No. 15JXN019). This study was supported partially by the Natural Science Foundation of China under Grant 61472090, Grant 61472089 and Grant 61672169, by the NSFC-Guangdong Joint Found U1501254, by the Guangdong Natural Science Funds for Distinguished Young Scholar under Grant S2013050014133, by the Natural Science Foundation of Guangdong under Grant 2015A030313486, by the Science and Technology Planning Project of Guangzhou under Grant 201707010492 and Grant 201604016041.

References

1 S. Lee, C. Khoo, C. W. Halstead, T. Huynh and A. Bensoussan, *J. AOAC Int.*, 2007, **90**, 1210–1218.
2 R. K. Gupta, *Vegetos*, 2008, **21**, 1–10.
3 N. P. Committee, *Pharmacopoeia of the People's Republic of China*, Chinese Medical Science and Technology Press, Beijing, 2010.
4 Q. F. Gong, *Science of Processing Chinese Materia Medica*, Chinese Medicine Press, Beijing, 2007.
5 T. B. o. d. a. o. t. P. s. R. o. China, *The Chinese Medicine Preparation Standards*, People's Medical Publishing House, Beijing, 1988.
6 D. J. Ye and S. T. Yuan, *Dictionary of Chinese Herbal Processing Science*, Shanghai Science and Technology Press, Shanghai, 2005.
7 M. Y. Mo, Q. H. Zhu and X. Y. Xue, *Chin. J. Exp. Tradit. Med. Formulae*, 2015, **21**, 1–4.
8 H. Wagner, *Phytomedicine*, 2006, **5**, 122–129.
9 G. R. Zimmermann, J. Lehár and C. T. Keith, *Drug Discovery Today*, 2007, **12**, 34–42.
10 E. Bellissant, V. Sébille and G. Paintaud, *Clin. Pharmacokinet.*, 1998, **35**, 151–166.
11 R. Q. Wu, *Strait Pharmaceutical Journal*, 2010, **22**, 26–28.
12 M. S. Li, X. Y. Huang, H. S. Liu, B. X. Liu, Y. Wu and L. J. Wang, *RSC Adv.*, 2015, **5**, 45520–45527.
13 F. Nilsson, K. Hallstensson, K. Johansson, Z. Umar and M. S. Hedenqvist, *Ind. Eng. Chem. Res.*, 2013, **52**, 8655–8663.
14 S. J. Zhou, J. Meng, Z. P. Huang, S. Z. Jiang and Y. Q. Tu, *Anal. Methods*, 2016, **8**, 2201–2206.
15 M. S. Li, X. Y. Huang, H. S. Liu, B. X. Liu, Y. Wu and F. R. Ai, *Acta Chim. Sin.*, 2013, **71**, 1053–1058.
16 X. L. Zhao, M. Turk, W. Li, K. C. Lien and G. Z. Wang, *Applied Soft Computing*, 2016, **48**, 151–159.
17 A. T. C. Goh, *Artif. Intell. Eng.*, 1995, **9**, 143–151.
18 D. S. Bro, *Complex Systems*, 1988, **2**, 321–355.
19 R. T. Xia and X. Y. Huang, *RSC Adv.*, 2015, **5**, 76979–76986.

20 M. S. Li, X. Y. Huang, H. S. Liu, B. X. Liu, Y. Wu, A. H. Xiong and T. W. Dong, *Fluid Phase Equilib.*, 2013, **356**, 11–17.
21 J. Nirmal, M. Zaveri, S. Patnaik and P. Kachare, *Applied Soft Computing*, 2014, **24**, 1–12.
22 D. F. Specht and H. Romsdahl, *IEEE World Congress on IEEE International Conference on Neural Networks*, 1994, **2**, 1203–1208.
23 C. Zhang, F. X. Cheng, W. H. Li, G. X. Liu, P. W. Lee and Y. Tang, *Mol. Inf.*, 2016, **35**, 136–144.
24 M. Paliwal and U. A. Kumar, *Applied Soft Computing*, 2011, **11**, 3690–3696.
25 M. Gevrey, I. Dimopoulos and S. Lek, *Ecol. Modell.*, 2003, **160**, 249–264.
26 J. D. Olden and D. A. Jackson, *Ecol. Modell.*, 2002, **154**, 135–150.
27 B. Kim, D. W. Lee, K. Y. Parka, S. R. Choi and S. Choi, *Vacuum*, 2004, **76**, 37–43.
28 J. D. Oña and C. Garrido, *Neural Comput. Appl.*, 2014, **25**, 859–869.
29 G. D. Garson, *Artificial Intelligence Expert*, 1991, **6**, 46–51.
30 L. Z. Yao, T. F. Li and J. Yi, *Computer Science*, 2012, **39**, 247–251.
31 D. F. Zhang, *Design and application of neural network*, Machinery Industry Press, Beijing, 2012.
32 X. Guo and K. Huang, *International Journal of Technology Management*, 2014, 131–134.